https://doi.org/10.5194/egusphere-2026-2597
Preprint. Discussion started: 20 May 2026

Atmospheric Rivers landfalling in Japan: Climatology and physical characteristics causing heavy rainfall

Yusuke Hiraga [1*], Sohta Tadaki [1], Ryotaro Tahara [1], Jose Angelo Hokson [2]

[1] Department of Civil and Environmental Engineering, Tohoku University, Sendai, Japan
[2] Department of Civil Engineering, FEATI University, Manila, Philippines

Correspondence to: Yusuke Hiraga (yusuke.hiraga.c3@tohoku.ac.jp)

Abstract. This study investigates the climatology and physical factors governing the precipitation efficiency of Atmospheric Rivers (ARs) landfalling in Japan. Using an ERA5 reanalysis-based AR database (1940–2023), we identified typical synoptic patterns of landfalling ARs via Self-Organizing Maps, which effectively categorize the regional moisture transport pathways. Climatological analysis revealed a significant increasing trend in AR frequency specifically in northern Japan. We further examined the relationship between AR characteristics and rainfall using nationwide high-resolution observations. While Integrated Water Vapor Transport (IVT) explains a substantial portion of the overall relationship (R = 0.71), considerable variability in precipitation amounts remains for similar IVT levels. Our analysis demonstrates that rainfall intensity is primarily modulated by a combination of strong moisture convergence (MVIMC), low convective inhibition (CIN), and orographic enhancement over high elevations. Furthermore, precipitable water (PW) emerged as the critical differentiator for the formation of quasi-stationary linear rainbands (QSLRBs), which consistently develop in close proximity to the AR axis. These findings suggest that the synoptic-scale AR provides the necessary environmental conditions for the organization of mesoscale extremes. Enhancing the predictive accuracy of AR landfall location and internal structure is thus a crucial prerequisite for improving the predictability of catastrophic localized rainfall in East Asia.

1 Introduction

Atmospheric Rivers (ARs) have gained significant attention as a key mechanism driving heavy precipitation events worldwide (Waliser and Guan, 2017; Payne et al., 2020; Stojanovic et al., 2026). Defined as long, narrow, and transient corridors of intense horizontal integrated water vapor transport (IVT), the AR concept is now widely applied in studies across the western United States and other regions frequently impacted by these features (Ralph et al., 2018).

Recent studies demonstrated that ARs are the primary drivers of flood damages in the western United States (Corringham et al., 2019). ARs are responsible for more than half of the annual maximum floods in a large portion of the central United States, significantly influencing the upper tail of flood peak distributions (Lavers and Villarini, 2013). In Western Europe, ARs have been shown to play a decisive role in shaping the upper tail of the extreme precipitation distribution (Lavers et al., 2011;

https://doi.org/10.5194/egusphere-2026-2597
Preprint. Discussion started: 20 May 2026

Lavers and Villarini, 2013; Ramos et al., 2015). In southwestern South America, top-quartile precipitation often occurs under AR conditions (Viale et al., 2018; Hiraga and Meza, 2025).

Across Asia, research has shown that ARs are responsible for a substantial portion (up to 90 %) of heavy rainfall events spanning the warm seasons (Kamae et al., 2017; Kim et al., 2021). Under a warming climate in East Asia, the intensification of AR and its rainfall is projected to drive a significant increase in the frequency of extreme events (Kamae et al., 2021). The strong association between ARs and high-impact, localized precipitation events has been reported in Japan (Hirota et al., 2016).

While the aforementioned studies have firmly established that ARs drive a substantial portion of extreme precipitation, their analyses primarily focus on quantifying the fraction of heavy rain events or annual maxima that coincide with ARs—effectively treating the presence of an AR as a sufficient condition for heavy rainfall. In other words, there is still a lack of AR-centric research aimed at identifying the specific physical characteristics that determine whether an AR will trigger high-impact, localized rainfall or pass without significant hydrologic consequences. While established frameworks, most notably the AR Scale (Ralph et al. 2019), categorize events based on bulk integrated metrics such as IVT and duration, such indices may not fully capture the thermodynamic and dynamic interactions—including static instability and localized moisture convergence—that determine whether an AR triggers catastrophic rainfall or passes with minimal hydrologic impact across the complex terrain of East Asia. Developing such a necessity-based analytical framework is essential for enhancing the predictive skill of extreme rainfall and for advancing our mechanistic understanding of the physical processes that govern AR-driven events.

Based on the above, this study aims to develop a necessity-based framework to identify the specific physical characteristics that determine the precipitation efficiency of ARs landfalling in Japan.

2 Materials and Methods

This study begins by characterizing the representative synoptic patterns and climatological frequency of landfalling ARs across Japan. Subsequently, we focus on the physical properties of ARs associated with precipitation in northwestern Japan (Fig. S1). This region was prioritized as our focal area due to the rising frequency of severe rainfall-driven disasters in recent years (Tochimoto and Hirockawa, 2024; Hiraga and Tahara, 2025a), combined with climate projections indicating further intensification of such extremes under a warming climate (Kawase et al., 2023). The following subsections detail the datasets and analytical procedures employed in this research.

2.1 Atmospheric River and associated atmospheric condition data

We used the global AR database based on Tracking Atmospheric Rivers Globally as Elongated Targets (tARget) algorithm version 4 on the ERA5 reanalysis (Guan and Waliser, 2024). This database provides global AR detection and tracking results at a 0.25° × 0.25° horizontal resolution and 6-hourly intervals covering the period from 1940 to 2023. The tARget v4 algorithm identifies ARs based on a combination of intensity (utilizing a location- and month-dependent 85th percentile IVT threshold

https://doi.org/10.5194/egusphere-2026-2597
Preprint. Discussion started: 20 May 2026

alongside a hemispheric lower limit), geometry (length > 2000 km and length-to-width ratio > 2), and direction requirements. Compared to previous versions, this regionally refined algorithm includes improved filtering of tropical cyclones and enhanced detection of "zonal" ARs and polar features, making it particularly robust for analyzing AR processes across diverse climatic zones (Guan and Waliser, 2024). The reliability and robustness of the tARget algorithm-based database in representing fundamental AR properties has been confirmed through several validation efforts comparing it with dropsonde and satellite-based observations (Yan et al., 2017; Eiras-Barca et al., 2018; Collow et al., 2022). We focused on the subset of ARs identified in the database that were associated with landfalls across Japan. To characterize the thermodynamic and dynamic environments associated with the identified ARs, we utilized a suite of ERA5-based variables and indices except for precipitation. Those include IVT, precipitable water, Convective Available Potential Energy (CAPE), Convective Inhibition (CIN), relative humidity, Mean Vertically Integrated Moisture Convergence (MVIMC), and elevation.

2.2 Radar/Raingauge-Analyzed Precipitation observation data

We used the Radar/Raingauge-Analyzed Precipitation observation data (RA data) as the ground-truth of precipitation over Japan (https://www.jma.go.jp/jma/kishou/know/kurashi/kaiseki.html). The RA data is a high-resolution gridded product that merges weather radar reflectivity with in-situ measurements. This dataset is generated by calibrating reflectivity from 46 C-band radars—operated by the Japan Meteorological Agency (JMA) and the Ministry of Land, Infrastructure, Transport, and Tourism (MLIT)—against a dense network of approximately 1,300 rain gauges, which have an average spacing of roughly 17 km. Owing to its fine spatial (1 km for 2006 onwards and 5 km for 1988-2006) and temporal (30-min) resolution, the RA data is widely regarded as a reliable ground-truth reference in Japan (Tsuguti et al., 2019; Hirockawa et al., 2020; Hiraga et al., 2026).

2.3 Experimental settings

Dominant trajectory patterns of ARs landfalling in Japan were classified using a Self-Organizing Map (SOM). SOM is an unsupervised neural network algorithm that projects high-dimensional input data onto a low-dimensional (typically two-dimensional) lattice while preserving topological relationships among data samples (Kalteh et al., 2008). This property makes SOM particularly suitable for classifying atmospheric circulation patterns and moisture transport pathways (i.e., Guirguis et al., 2019; Ramseyer et al., 2022). The SOM analysis was performed using the MiniSom package in Python. As input data, we used the zonal and meridional components of IVT at the representative timing of each AR event. Prior to training, both components were normalized to ensure equal weighting in the clustering process. The SOM was trained for 10,000 iterations with a learning rate of 0.3 and an initial neighborhood radius of 1.0. Through this process, AR events with similar IVT direction and magnitude are grouped together, yielding distinct AR trajectory clusters.

Long-term trends in landfalling AR frequency over Japan were evaluated using the Mann–Kendall test, a widely used non-parametric statistical method for detecting monotonic trends in hydro-climatological time series (Da Silva et al., 2015; Wang et al., 2020). The Mann–Kendall test was selected because it does not assume a normal distribution of the data and is robust

https://doi.org/10.5194/egusphere-2026-2597
Preprint. Discussion started: 20 May 2026

against outliers and missing values, making it well suited for analyzing climate-related event frequencies. The analysis was conducted using the pymannkendall package in Python (Hussain and Mahmud, 2019). The non-parametric Mann–Kendall test was applied to the 1940–2023 time series of annual AR frequency at a 0.25° × 0.25° grid resolution across Japan.

2.4 Relationship between AR characteristics and precipitation

We first identified AR events whose shapes intersected northwestern Japan (target area for precipitation analysis). For each 6-hourly time step within an event, all meteorological variables were spatially constrained to the intersection of the AR shape and the target region. To derive representative characteristics for each event, these variables were temporally aggregated—via averaging or accumulation—across the event's duration. Regarding precipitation, we applied a 1-mm threshold to the event-total accumulation to exclude minor rainfall and isolate the signal directly associated with AR activity. Finally, these fields were spatially averaged to yield a single scalar value per AR event for each physical variable. We first examined the relationship between IVT and event-total precipitation, as previous studies have demonstrated that high IVT is a primary driver of extreme rainfall and flood-producing events (e.g., Guan et al. 2023). To further investigate the precipitation variability that remains unexplained by IVT, we refined our dataset by excluding events with minimal influence on northwestern Japan. This was achieved using two filters: (1) removing events with IVT below the 30th percentile, and (2) excluding events where the spatial overlap between the AR footprint and the study area was below the 10th percentile. As a result, 251 events were removed, leaving 479 events for robust statistical modeling. To objectively distinguish between AR events that were exceptionally efficient at producing rainfall and those that were not, we applied Huber regression (Sun et al., 2020) to the remaining 479 events. Unlike ordinary least squares regression, Huber regression is less sensitive to outliers by combining squared-error loss for small residuals with absolute-error loss for large residuals. This approach is particularly advantageous for precipitation data, which typically exhibit heavy tails due to extreme rainfall events. Using the HuberRegressor from the scikit-learn library (Pedregosa et al., 2011), we established a baseline relationship. We then defined positive residual events and negative residual events as those exceeding the 80th percentile and falling below the 20th percentile of the residual distribution, respectively. The positive residual group represents cases where precipitation was substantially larger than expected from IVT alone, whereas the negative residual group represents cases with unexpectedly weak precipitation despite significant moisture transport.

We also focus on quasi-stationary linear rainbands (QSLRB), referred to as “Senjo-Kousuitai” in Japanese (Kato, 2020), as regional important precipitation events. In Japan, these quasi-stationary linear rainbands are the primary drivers of recent catastrophic rainfall events, accounting for over 60% of hydro-meteorological disasters when excluding those associated with tropical cyclones (Tsuguti and Kato 2014). QSLRB in northwestern Japan were identified using a spatio-temporal object-tracking algorithm proposed by Hirockawa et al. (2020). Briefly, spatially contiguous rainfall areas were first detected at each time step and subsequently aggregated into single heavy rainfall events based on their temporal overlap (at least 40%). This procedure effectively captures quasi-stationary systems that persist over time with minimal spatial displacement. To isolate linear systems, we evaluated the geometric properties of these heavy rainfall events, classifying them as QSLRB when they

https://doi.org/10.5194/egusphere-2026-2597
Preprint. Discussion started: 20 May 2026

satisfied a linearity criterion (aspect ratio >= 2.5). Detailed descriptions of the detection thresholds and geometric calculations are provided in the Appendix. The extracted QSLRB events were then compared with AR events identified using the tARget algorithm. A QSLRB was considered to be associated with an AR when its occurrence overlapped temporally with the AR during its lifetime.

3 Results

3.1 Characterizing the representative synoptic patterns and climatological frequency of landfalling ARs across Japan

3.1.1. Representative synoptic patterns

From the full AR database spanning 1940–2023, a total of 22,634 six-hourly AR detections were found to spatially overlap with the Japan island. In this study, we focus on June–August, when heavy rainfall events frequently occur in Japan. Restricting the analysis to these months reduces the number of AR timings to 9,037. A single representative timing was selected for each AR event based on the maximum spatial overlap with Japan, yielding a total of 1,775 AR events used for the climatological analyses.

Our SOM-based analysis revealed distinct AR patterns landfalling in Japan (Figure 1). Figure 1 presents the composites of IVT fields for the four resulting clusters (A-D). The sample size (n) and the percentage of total AR events are indicated above each panel. Bottom row of Figure 1 shows representative snapshots of individual AR events corresponding to each cluster; shading represents IVT magnitude, green contours delineate the detected AR footprints, and yellow dashed lines indicate the AR axes. The date and time of each detected event are shown above the panels. After testing multiple SOM configurations, a 2 × 2 node structure was selected, as it provided the clearest separation of physically interpretable AR trajectory types while avoiding excessive fragmentation. Cluster D is the most frequent, making up to 44.7% of all AR events landfalling in Japan, characterized by strong moisture transport directly landfalling on Kyushu and extending northeastward over the main island of Japan. These events typically represent the narrow, elongated synoptic jets of water vapor. Such configuration of water vapor transport is frequently coupled with frontal systems in the region, a relationship long recognized in previous studies (e.g., Matsumoto et al. 1971). Clusters A and C exhibit similar flow orientations, characterized by moisture transport originating from the south and progressing northward while curving eastward. This configuration reflects the influence of the Western North Pacific Subtropical High (WNPSH) situated to the east, with moisture being channeled along the anticyclonic periphery of the high-pressure system (e.g., Zhao et al., 2022). The distinctions between Clusters A and C represent shifts in the moisture transport axis resulting from the longitudinal displacement of the WNPSH. Specifically, the westward extension of the WNPSH in Cluster C appears to be a critical condition for directing intense moisture transport into northern Japan. Cluster B is characterized by a zonal AR pattern, where a strong meridional (north-south) pressure gradient drives dominant westerly winds (zonal flow) along the subtropical jet stream (Mundhenk et al., 2016). This results in a concentrated and intense IVT core that extends nearly parallel to the southern coast of Japan. In this cluster, moisture transport takes the form of potent but often rapidly moving filaments. The tARget v4 algorithm is specifically refined to identify such

https://doi.org/10.5194/egusphere-2026-2597
Preprint. Discussion started: 20 May 2026

zonal orientations by evaluating poleward requirements based on segments of the AR axis rather than the entire object (Guan and Waliser, 2024).

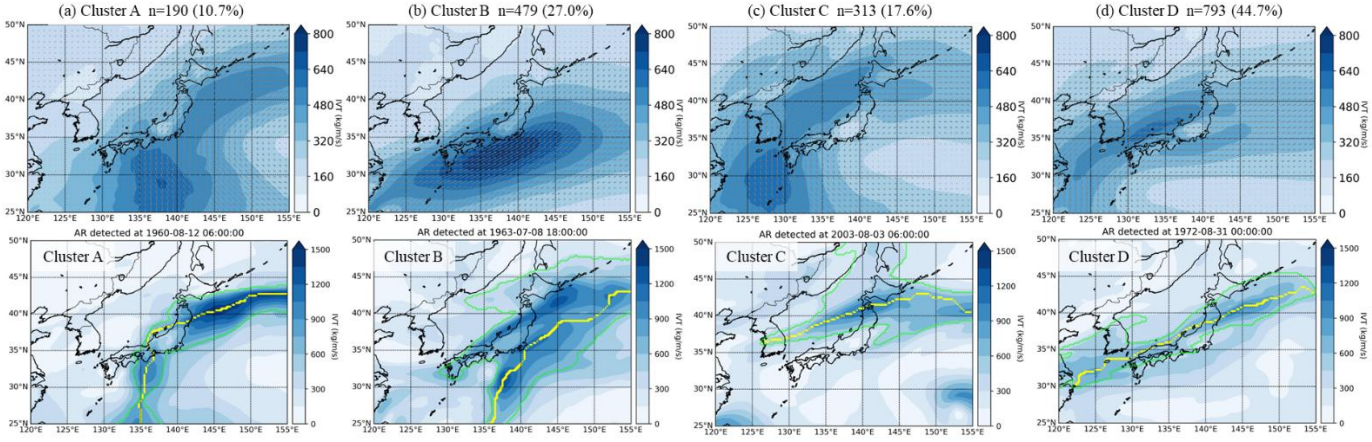

Figure 1 Classification of landfalling ARs over Japan using SOM. (Top row) Composite mean of IVT; vectors and shading, kgm^{-1}s^{-1}) for Clusters A–D based on the maximum spatial overlap timing with Japan. (Bottom row) Representative snapshots of individual AR events corresponding to each cluster.

3.1.2. Climatological frequency and trend of landfalling ARs

Based on the extracted subset of 1,775 AR events landfalling in Japan, we examined the annual frequency and duration of AR events at each grid point in Japan (Figure 2). The spatial distribution of the annual AR frequency (Figure 2a) reveals that Japan is frequently influenced by ARs, with most regions experiencing 15 to 25 events per year. The highest frequencies are concentrated along the Honshu island, particularly from Central Japan to the Tohoku region (35°N-42°N), where the values exceed 20 events per year. Southern Japan (Kyushu Island) exhibits a unique characteristic where a lower annual frequency is offset by a notably higher duration per event (Figure 2b), indicating that while AR landfalls are less frequent in this area, their influence is more persistent once an event is initiated. Regarding the average duration of AR events (Figure 2b), the results show that once an AR influences a grid cell, its impact typically persists for 10 to 13.5 hours. As mentioned, the longest durations (exceeding 12.5 to 13 hours per event) are concentrated in Kyushu Island. This prolonged influence suggests that ARs in this region may be associated with slow-moving synoptic systems or quasi-stationary moisture transport patterns, such as those linked to the Meiyu-Baiu front. In higher latitudes, the longer durations may also be attributed to the larger spatial scales of AR footprints as they progress northeastward along Japan. The trend analysis of annual AR frequency from 1940 to 2023 (Figure 2c) highlights a significant regional intensification of AR activity. A marked increasing trend is clearly identified in the northern half of Japan, covering a large part of Tohoku, with positive slopes reaching 0.13 to 0.17 events per year. These trends are statistically significant, indicating that the frequency of AR landfalls in this specific region has increased by approximately 10 to 13 events over the 84-year study period. This localized increase in AR frequency in northern Japan is particularly noteworthy as it aligns with the recent rise in extreme precipitation events and associated disasters in this area.

https://doi.org/10.5194/egusphere-2026-2597
Preprint. Discussion started: 20 May 2026

Figure 2d further illustrates the temporal characteristics of AR events landfalling in Japan, interannual variability of the annual occurrence frequency for each AR cluster from 1940 to 2023. The total number of landfalling ARs fluctuates between approximately 15 and 30 events per year, with Cluster D consistently serving as the most dominant contributor throughout the study period. While substantial year-to-year variability is evident across all categories, no statistically significant long-term trends were identified for any individual cluster. This lack of a clear trend at the cluster-wide level suggests that the localized increasing trend in AR frequency observed in northern Japan (as shown in Figure 2c) may not be driven by a simple increase in the occurrence of a specific AR type. Instead, it likely reflects more complex shifts in the spatial distribution of AR tracks or changes in the internal structure and intensity of events within these clusters over time.

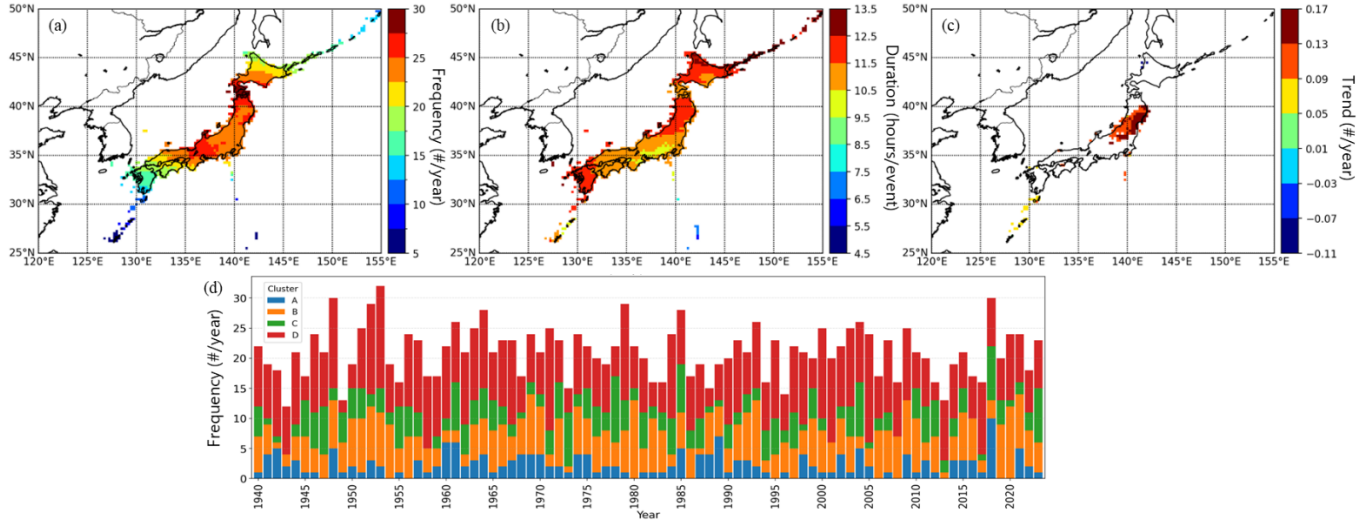

Figure 2 Climatology and long-term trends of landfalling ARs over Japan (1940–2023). Maps show (a) annual frequency of AR events (#/year), (b) mean duration per AR event (hours/event), and (c) the trend (Sen's slope) in annual AR frequency (#/year). In (c), only trends that are statistically significant ($p < 0.05$) are shown. (d) Stacked bar chart showing the total annual frequency of AR events in Japan from 1940 to 2023, broken down by SOM-derived cluster types (A, B, C, D) as defined in Figure 1.

3.2 Relationship between AR characteristics and precipitation

3.2.1. AR characteristics linked to heavy precipitation

Figure 3a illustrates the scatter relationship between event-accumulated IVT and precipitation associated with individual AR events. Each point represents the representative values for a single AR event. The Pearson correlation coefficient was 0.71 ($p < 0.001$), indicating a statistically significant and strong positive relationship. However, despite this overall correlation, the considerable dispersion in precipitation amounts for similar IVT levels suggests that moisture transport alone is a necessary but not sufficient condition for determining the intensity of AR-related rainfall. Notably, some events with high IVT resulted in relatively minor precipitation, whereas others with moderate IVT triggered extreme rainfall, highlighting the role of

https://doi.org/10.5194/egusphere-2026-2597
Preprint. Discussion started: 20 May 2026

additional dynamical or thermodynamical factors. Figure 3b shows the fitted Huber regression line (solid) and the 80th percentile residual bounds (dashed), which facilitate the objective classification of events into "positive residual" (red) and "negative residual" (blue) groups. The positive residual group consists of 46 events where precipitation significantly exceeded the amount predicted by IVT alone, while the negative residual group includes 50 events where rainfall was unexpectedly weak despite substantial moisture transport. This classification enables a comparative analysis of AR events with similar moisture intensities but contrasting hydrological outcomes, thereby isolating the additional meteorological factors that drive extreme rainfall efficiency.

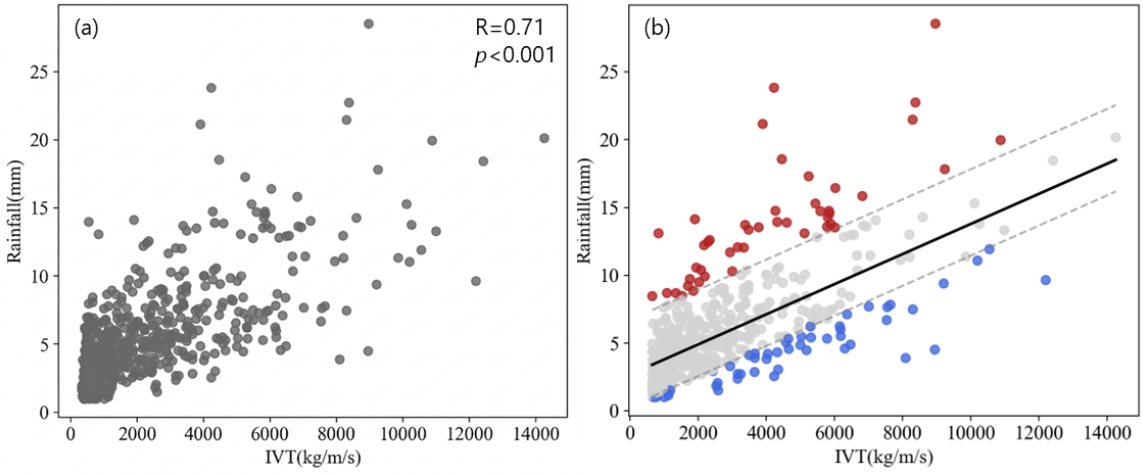

Figure 3 Relationship between event-accumulated precipitation and accumulated IVT for AR events landfalling in northwestern Japan. (a) Scatter plot of precipitation versus IVT, with the pearson correlation coefficient (R) and p-value indicated in the upper right. (b) Huber robust regression analysis for the objective classification of events. The solid line indicates the fitted regression line, and the dashed lines denote the 80th percentile bounds of the residuals. Red (blue) points represent positive (negative) residual events.

Figure 4 shows the spatio-temporal mean values of meteorological and static variables—calculated over the intersection of the AR footprint and northwestern Japan—for the positive (red) and negative (blue) residual groups. Variables were calculated over the intersection of the AR footprint and northwestern Japan for the positive (red) and negative (blue) residual groups. As intended by our regression-based classification, IVT ($p = 0.16$) and Precipitable Water (PW; $p = 0.61$) show no significant differences between the two groups. This confirms that the contrast in rainfall efficiency is not primarily driven by the magnitude of the total moisture supply or the total column water vapor. Similarly, CAPE does not exhibit a significant difference ($p = 0.92$), suggesting that the available potential energy for convection was comparable in both cases. In contrast, several key variables show highly significant differences that explain the higher precipitation efficiency in the positive group. The MVIMC is significantly larger in the positive group (Figure 4a), indicating that stronger convergence within AR footprint is a primary driver of enhanced rainfall. Furthermore, the positive group is characterized by significantly lower CIN (Figure 4d) and higher mid-level humidity (RH at 500hPa; Figure 4f). These conditions suggest an environment where deep convection

https://doi.org/10.5194/egusphere-2026-2597
Preprint. Discussion started: 20 May 2026

is more easily triggered and less prone to the detrimental effects of dry-air entrainment. Geographical and static factors also provide critical insights. The Mean Latitude of the AR axis (Figure 4g) is significantly lower for the positive group, implying that ARs positioned further south—closer to the warm and moist air masses of the subtropical high—are more likely to produce heavy rainfall in this region. Notably, Landfalling Elevation (Figure 4j) is markedly higher for the positive group, strongly suggesting that orographic enhancement is a decisive mechanism for maximizing precipitation as moist air is forced to ascend over higher terrain. Finally, the scale and persistence of the AR events appear to have a minimal role in determining rainfall efficiency. Neither AR duration ($p = 0.46$) nor overlap percentage ($p = 0.18$) shows a statistically significant difference between the two groups. This indicates that heavy rainfall in northwestern Japan is primarily governed by dynamical forcing (convergence and orography) and the vertical structure of the atmosphere (stability and humidity) rather than the temporal duration or spatial extent of the AR impact.

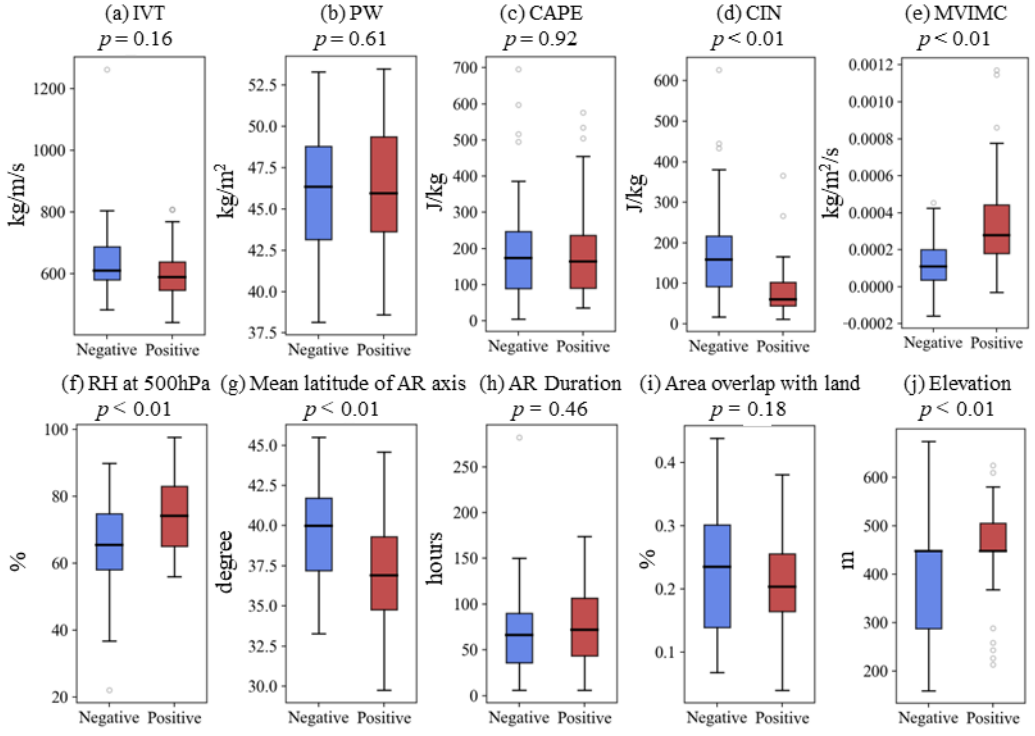

Figure 4 Comparison of meteorological and static variables between the positive and negative residual groups. Box plots show the spatio-temporal mean values of (a) IVT, (b) PW, (c) CAPE, (d) CIN, (e) MVIMC, (f) RH at 500hPa, (g) mean latitude of the AR axis, (h) AR duration, (i) area overlap with land, and (j) landfalling elevation.

3.2.2 AR characteristics linked to QSLRB

Among the 243 AR events landfalling in the target area (northwestern Japan) analyzed during the 2006–2023 period, 47 events (19.34%) were associated with at least one detected QSLRB, while 196 events (80.66%) were not. To robustly compare

https://doi.org/10.5194/egusphere-2026-2597
Preprint. Discussion started: 20 May 2026

the environmental characteristics favoring QSLRB formation, we excluded AR events with total precipitation lower than the 20th percentile of the QSLRB-associated group (6.72 mm). This filtering process ensures that both groups are compared under broadly similar rainfall intensities, allowing us to isolate the specific atmospheric factors that facilitate the organization of convection into quasi-stationary linear systems rather than simply measuring the total moisture volume.

The composite IVT maps (Figures 5a and 5b) reveal distinct structural differences between the two groups. For AR events associated with QSLRBs (Figure 5b), the moisture flux is markedly stronger over the northern Japan Sea compared to those without QSLRBs (Figure 5a). This intensified flux is directed more precisely toward northwestern Japan, delivering a more concentrated stream of water vapor to the target region. This configuration appears to be driven by a stronger westward extension of the WNPSH, which acts as a dynamic barrier and channels the moisture northward along its western periphery. Additionally, the eastward moisture transport exiting over northern Japan is also more pronounced in the QSLRB group, indicating a well-defined and deep moisture highway across the archipelago.

Statistical analysis of the meteorological variables shown in Figure 4 identifies PW as the primary differentiator. Among all evaluated parameters, PW was the only variable that exhibited a statistically significant difference between AR events with and without QSLRBs (Figure 5c). This suggests that for AR events with comparable rainfall potential, a higher background concentration of PW in the target region is a critical precursor for QSLRB development.

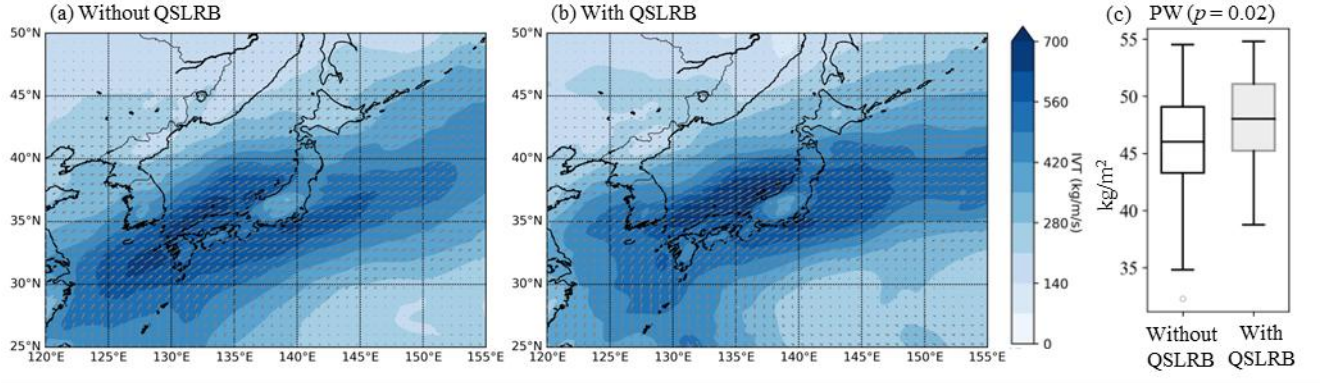

Figure 5 Composite mean IVT (vectors and shading, $kgm^{-1}s^{-1}$) for rainfall-matched events (a) without QSLRBs and (b) with QSLRBs; (c) Box plots comparing Precipitable Water (PW, kgm^{-2}) between the two groups.

Figure 6 shows representative patterns of AR-induced QSLRBs in northwestern Japan. In these snapshots, the red contours (perimeter of QSLRB) are consistently identified in close spatial proximity to the AR axis (yellow dashed line), which represents the core of the IVT maximum. Whether the AR exhibits a zonal orientation (Figures 6a and 6b) or a more curved synoptic structure (Figures 6c and 6d), the initiation and maintenance of disastrous QSLRBs appear to be intrinsically linked to the high-IVT filament of the AR. A recurring pattern in these events is that QSLRBs are predominantly aligned with the primary AR axis, typically located slightly to the south of the axis or directly aligned with it. This spatial alignment suggests that the AR axis acts as a moisture highway that provides the continuous, concentrated water vapor supply necessary to sustain

https://doi.org/10.5194/egusphere-2026-2597
Preprint. Discussion started: 20 May 2026

back-building or training convective processes. The synoptic-scale AR effectively provides the necessary environmental scaffolding—including low-level convergence and a moistened atmosphere—within which mesoscale extreme rainfall systems can organize and persist.

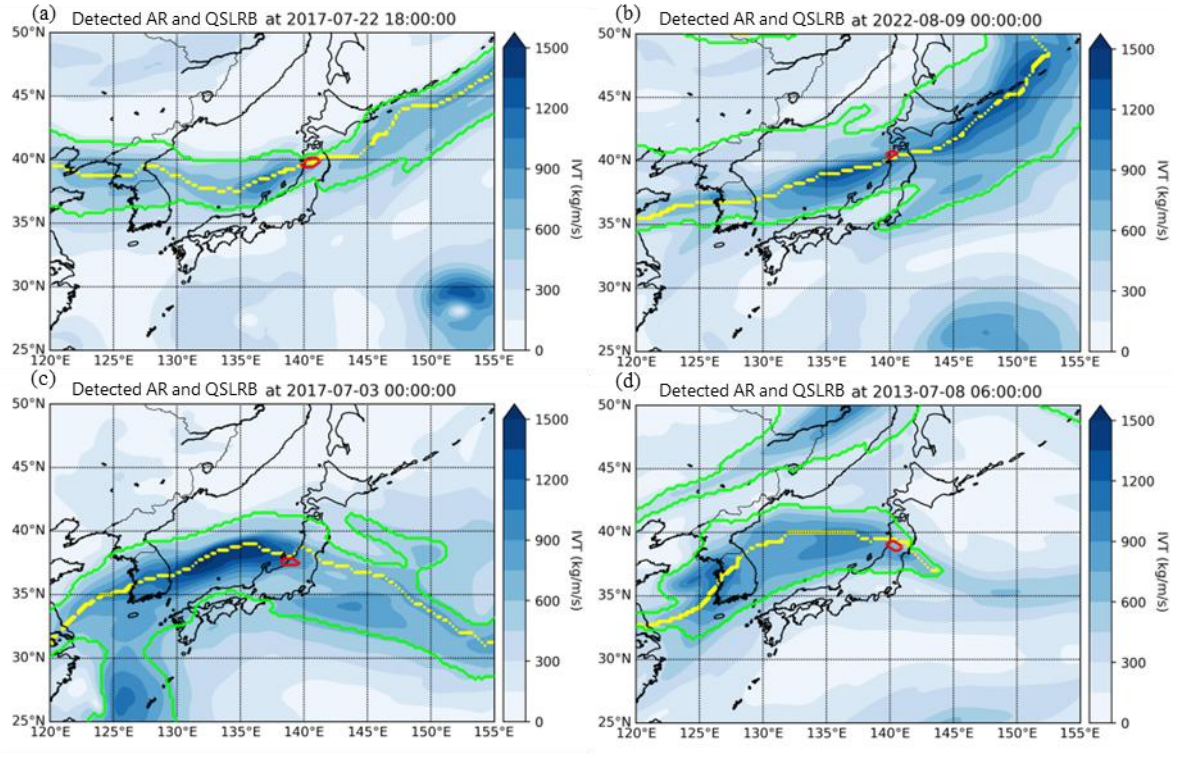

Figure 6 Representative snapshots of ARs and Quasi-Stationary Linear Rainbands (QSLRBs) occurring simultaneously. Contours indicate the detected AR shape (green), the AR axis (yellow dashed line), and the QSLRB outline (red).

4 Discussion

The identified increasing trend in the annual frequency of ARs in northwestern Japan (0.13–0.17 events/year; Figure 2c) is particularly noteworthy. Despite the lack of long-term trends in individual AR clusters (Figure 2d), the spatial concentration of these events over northwestern Japan suggests a systematic shift in their tracks. This observational evidence aligns with projections by Kamae et al. (2021), who argued that enhanced moisture flux and changing pressure gradients under a warming climate would lead to more frequent and intense AR impacts in East Asia.

The decoupling between the magnitude of IVT and rainfall intensity (Figure 3a) underscores that heavy precipitation is not merely a product of moisture transport amount. Our analysis identifies MVIMC and CIN as critical modulators of this rainfall efficiency. The importance of strong convergence for regional heavy rainfall is well aligned with previous studies (Hirota et al., 2016; Tsuji et al., 2021; Hiraga and Tahara, 2025a; 2025b), suggesting the intersection of high-IVT filaments with low-

https://doi.org/10.5194/egusphere-2026-2597
Preprint. Discussion started: 20 May 2026

level wind convergence zones is a prerequisite for localized high-impact events. Furthermore, the significantly lower CIN in the positive residual group indicates that the absence of a convective inhibition allows the moisture fed by the AR to be released as deep convection more effectively. This is further supported by the high mid-level moisture (Figure 4h) whose importance has been emphasized in recent studies (Zhang et al., 2019; Kato et al., 2024; Yoshida et al., 2025). The decisive role of landfalling elevation confirms that orographic enhancement is a primary necessity factor for northwestern Japan—a finding that complements the East Asian dynamics described by Park et al. (2021).

A key distinction of this study is the identification of PW as the sole significant differentiator for the formation of QSLRBs (Figure 5d). While IVT and MVIMC provide dynamic forcing, a high background of PW is essential for the organization and maintenance of these systems. Environments with high PW allows convective cells to maintain their organization and support the back-building or training processes necessary for the persistence of QSLRBs (Takahashi and Fujinami 2021). Furthermore, our findings suggest that because disastrous mesoscale systems like QSLRBs locate proximity to axis of synoptic-scale moisture transport, enhancing the forecast accuracy of ARs—specifically their exact landfall location, orientation, and timing—is a crucial prerequisite for improving the predictability of mesoscale extreme rainfall events. While QSLRBs themselves remain challenging to forecast due to their small-scale stochastic nature (Hatsuzuka et al., 2022), the high spatial correlation between the AR axis and QSLRB occurrence demonstrated in Figure 6 indicates that synoptic AR monitoring can serve as a robust precursor for identifying high-risk areas for devastating rainfall.

While this study offers a novel necessity-based framework, some limitations remain. First, the 0.25° resolution of the ERA5 reanalysis may not adequately resolve local-scale moisture transport influenced by Japan's complex topography. Given that heavy rainfall events—and specifically QSLRBs—can be driven by moisture flux channeled through narrow terrain features, utilizing higher-resolution datasets or cloud-resolving regional models is crucial for capturing these fine-scale interactions within the AR scaffolding. Second, our analysis focused on event-integrated metrics to define residual groups. However, the internal temporal evolution of an AR—such as the rapid intensification of IVT or shifting wind directions during landfall—could also play a role in triggering extremes. Future studies should investigate the sub-event scale dynamics to refine the predictive precursors identified here. Finally, while we established clear observational trends, the underlying causal links between specific background anomalies (e.g., Sea Surface Temperature) and the shifting AR tracks warrant further investigation to improve long-range seasonal forecasting for the region.

5 Conclusion

The key findings of this research are summarized as follows:

- A significant increasing trend in the annual frequency of ARs was identified in northwestern Japan from 1940 to 2023, highlighting shifting hydrometeorological risks in this area.

https://doi.org/10.5194/egusphere-2026-2597
Preprint. Discussion started: 20 May 2026

- Using Self-Organizing Maps (SOM), typical synoptic configurations of landfalling ARs were organized into distinct clusters, providing a structured baseline for assessing the meteorological variability of moisture transport patterns affecting Japan.
- The decoupling between IVT magnitude and rainfall intensity confirms that moisture transport is a necessary but not sufficient condition; instead, AR precipitation efficiency is governed by specific necessity factors, including stronger moisture convergence (MVIMC), lower convective inhibition (CIN), and significant orographic enhancement over higher landfalling elevations.
- Among various state variables, PW emerged as the sole significant differentiator for the formation of QSLRBs, where high background moisture is essential for maintaining the organization of linear convective systems.
- Disastrous QSLRBs are consistently located near the AR axis, where the synoptic-scale environment supports their formation.

By isolating these physical precursors, this study advances our understanding of AR-driven heavy rainfall events and underscores that enhancing the predictive accuracy of AR landfall and its internal structure—specifically its location, orientation, and timing—is a crucial prerequisite for improving the predictability of localized catastrophic rainfall in Japan.

Code availability

The codes can be provided from the corresponding author upon a reasonable request.

Data availability

Global Atmospheric River Database version 4 is available at (https://doi.org/10.25346/S6/ZSW7UN). Radar/Raingauge-Analyzed Precipitation observation data may be purchased from Japan Meteorological Business Support Center (https://www.jmbsc.or.jp/jp/offline/cd0100.html). Our analysis results can be provided by the corresponding author upon a reasonable request.

Author contributions

Y.H.: Conceptualization, Methodology, Software, Funding acquisition, Supervision, Writing (original Draft); S.T.: Methodology, Formal Analysis, Investigation, Data Curation, Visualization, Writing (review and editing); R.T.: Methodology, Formal Analysis, Writing (review and editing); J.A.H.: Data Curation, Supervision, Writing (review and editing)

Competing interests

The authors declare that they have no conflict of interest

https://doi.org/10.5194/egusphere-2026-2597
Preprint. Discussion started: 20 May 2026

Acknowledgements

This work was supported by JSPS KAKENHI Grant Number 24K17350.

References

1) Collow, A. M., Shields, C. A., Guan, B., Kim, S., Lora, J. M., McClenny, E. E., ... & Wehner, M. (2022). An overview of ARTMIP's Tier 2 Reanalysis Intercomparison: Uncertainty in the detection of atmospheric rivers and their associated precipitation. Journal of Geophysical Research: Atmospheres, 127(8), e2021JD036155.

2) Corringham, T. W., Ralph, F. M., Gershunov, A., Cayan, D. R., & Talbot, C. A. (2019). Atmospheric rivers drive flood damages in the western United States. Science advances, 5(12), eaax4631.

3) Da Silva, R. M., Santos, C. A., Moreira, M., Corte-Real, J., Silva, V. C., & Medeiros, I. C. (2015). Rainfall and river flow trends using Mann–Kendall and Sen's slope estimator statistical tests in the Cobres River basin. Natural Hazards, 77(2), 1205-1221.

4) Eiras-Barca, J., Ramos, A. M., Pinto, J. G., Trigo, R. M., Liberato, M. L., & Miguez-Macho, G. (2018). The concurrence of atmospheric rivers and explosive cyclogenesis in the North Atlantic and North Pacific basins. Earth System Dynamics, 9(1), 91-102.

5) Guan, B., & Waliser, D. E. (2024). A regionally refined quarter-degree global atmospheric rivers database based on ERA5. Scientific Data, 11(1), 440.

6) Guirguis, K., Gershunov, A., Shulgina, T., Clemesha, R. E., & Ralph, F. M. (2019). Atmospheric rivers impacting Northern California and their modulation by a variable climate. Climate Dynamics, 52(11), 6569-6583.

7) Hatsuzuka, D., Ryohei, K. A. T. O., Shimizu, S., & Shimose, K. I. (2022). Verification of forecasted three-hour accumulated precipitation associated with "senjo-kousuitai" from very-short-range forecasting operated by the JMA. Journal of the Meteorological Society of Japan. Ser. II, 100(6), 995-1005.

8) Hiraga, Y., & Tahara, R. (2025a). Sensitivity of localized heavy rainfall in Northern Japan to WRF physics parameterization schemes. Atmospheric Research, 314, 107802.

9) Hiraga, Y., & Tahara, R. (2025b). Responses of Convective Heavy Rainfall to Atmospheric Moisture Amplification: Implications for Probable Maximum Precipitation (PMP) Estimation. Journal of Hydrometeorology, 26(8), 1037-1052.

https://doi.org/10.5194/egusphere-2026-2597
Preprint. Discussion started: 20 May 2026

10) Hiraga, Y., Mbugua, J. M., Kotsuki, S., Suzuki, Y., Chen, S. H., Hamada, A., ... & Funatomi, T. (2026). Numerical experiments of cloud seeding for mitigating localization of heavy rainfall: a case study of Mesoscale Convective System in Japan. Natural Hazards and Earth System Sciences, 26(3), 1287-1303.

11) Hirockawa, Y., Kato, T., Araki, K., & Mashiko, W. (2020a). Characteristics of an extreme rainfall event in Kyushu district, southwestern Japan in early July 2020. SOLA, 16, 265-270.

12) Hirockawa, Y., Kato, T., Tsuguti, H., & Seino, N. (2020b). Identification and classification of heavy rainfall areas and their characteristic features in Japan. Journal of the Meteorological Society of Japan. Ser. II, 98(4), 835-857.

13) Hirota, N., Takayabu, Y. N., Kato, M., & Arakane, S. (2016). Roles of an atmospheric river and a cutoff low in the extreme precipitation event in Hiroshima on 19 August 2014. Monthly Weather Review, 144(3), 1145-1160.

14) Hussain, M., & Mahmud, I. (2019). pyMannKendall: a python package for non parametric Mann Kendall family of trend tests. Journal of open source software, 4(39), 1556.

15) Kalteh, A. M., Hjorth, P., & Berndtsson, R. (2008). Review of the self-organizing map (SOM) approach in water resources: Analysis, modelling and application. Environmental Modelling & Software, 23(7), 835-845.

16) Kamae, Y., Imada, Y., Kawase, H., & Mei, W. (2021). Atmospheric rivers bring more frequent and intense extreme rainfall events over East Asia under global warming. Geophysical Research Letters, 48(24), e2021GL096030.

17) Kamae, Y., Mei, W., & Xie, S. P. (2017). Climatological relationship between warm season atmospheric rivers and heavy rainfall over East Asia. Journal of the Meteorological Society of Japan. Ser. II, 95(6), 411-431.

18) Kato, R., Shimizu, S., Shimose, K. I., Hirano, K., Shiraishi, K., Yoshida, S., ... & Nagai, T. (2024). Improvement of two-hour-ahead QPF using blending technique with spatial maximum filter for tolerating forecast displacement errors and water vapor lidar assimilation. Journal of the Meteorological Society of Japan. Ser. II, 102(4), 445-464.

19) Kato, T. (2020). Quasi-stationary band-shaped precipitation systems, named “Senjo-Kousuitai”, causing localized heavy rainfall in Japan. Journal of the Meteorological Society of Japan. Ser. II, 98(3), 485-509.

20) Kawase, H., Nosaka, M., Watanabe, S. I., Yamamoto, K., Shimura, T., Naka, Y., ... & Takayabu, I. (2023). Identifying robust changes of extreme precipitation in Japan from large ensemble 5-km-Grid regional experiments for 4K warming scenario. Journal of Geophysical Research: Atmospheres, 128(18), e2023JD038513.

https://doi.org/10.5194/egusphere-2026-2597
Preprint. Discussion started: 20 May 2026

21) Kim, J., Moon, H., Guan, B., Waliser, D. E., Choi, J., Gu, T. Y., & Byun, Y. H. (2021). Precipitation characteristics related to atmospheric rivers in East Asia. Int. J. Climatol, 41, E2244-E2257.

22) Lavers, D. A., Allan, R. P., Wood, E. F., Villarini, G., Brayshaw, D. J., & Wade, A. J. (2011). Winter floods in Britain are connected to atmospheric rivers. Geophysical Research Letters, 38(23).

23) Lavers, D. A., & Villarini, G. (2013a). Atmospheric rivers and flooding over the central United States. Journal of Climate, 26(20), 7829-7836.

24) Lavers, D. A., & Villarini, G. (2013b). The nexus between atmospheric rivers and extreme precipitation across Europe. Geophysical Research Letters, 40(12), 3259-3264.

25) Matsumoto, S., Ninomiya, K., & Yoshizumi, S. (1971). Characteristic features of "Baiu" front associated with heavy rainfall. Journal of the Meteorological Society of Japan. Ser. II, 49(4), 267-281.

26) Mundhenk, B. D., Barnes, E. A., & Maloney, E. D. (2016). All-season climatology and variability of atmospheric river frequencies over the North Pacific. Journal of Climate, 29(13), 4885-4903.

27) Park, C., Son, S. W., & Kim, H. (2021). Distinct features of atmospheric rivers in the early versus late East Asian summer monsoon and their impacts on monsoon rainfall. Journal of Geophysical Research: Atmospheres, 126(7), e2020JD033537.

28) Payne, A. E., Demory, M. E., Leung, L. R., Ramos, A. M., Shields, C. A., Rutz, J. J., ... & Ralph, F. M. (2020). Responses and impacts of atmospheric rivers to climate change. Nature Reviews Earth & Environment, 1(3), 143-157.

29) Pedregosa, F., Varoquaux, G., Gramfort, A., Michel, V., Thirion, B., Grisel, O., ... & Duchesnay, É. (2011). Scikit-learn: Machine learning in Python. the Journal of machine Learning research, 12, 2825-2830.

30) Ralph, F. M., Dettinger, M. D., Cairns, M. M., Galarneau, T. J., & Eylander, J. (2018). Defining "atmospheric river": How the Glossary of Meteorology helped resolve a debate. Bulletin of the American Meteorological Society, 99(4), 837-839.

31) Ralph, F. M., Rutz, J. J., Cordeira, J. M., Dettinger, M., Anderson, M., Reynolds, D., ... & Smallcomb, C. (2019). A scale to characterize the strength and impacts of atmospheric rivers. Bulletin of the American Meteorological Society, 100(2), 269-289.

32) Ramos, A. M., Trigo, R. M., Liberato, M. L., & Tomé, R. (2015). Daily precipitation extreme events in the Iberian Peninsula and its association with atmospheric rivers. Journal of Hydrometeorology, 16(2), 579-597.

https://doi.org/10.5194/egusphere-2026-2597
Preprint. Discussion started: 20 May 2026

33) Ramseyer, C. A., Stanfield, T. J., Van Tol, Z., Gingrich, T., Henry, P., Forister, P., ... & Sauda, S. S. (2022). Identifying Eastern US atmospheric river types and evaluating historical trends. Journal of Geophysical Research: Atmospheres, 127(17), e2021JD036198.

34) Stojanovic, M., Pérez-Alarcón, A., Sorí, R., Nieto, R., & Gimeno, L. (2026). Atmospheric rivers are associated with nine out of every 10 floods in major global river basins. npj Natural Hazards, 3(1), 6.

35) Sun, Q., Zhou, W. X., & Fan, J. (2020). Adaptive huber regression. Journal of the American Statistical Association, 115(529), 254-265.

36) Takahashi, H. G., & Fujinami, H. (2021). Recent decadal enhancement of Meiyu–Baiu heavy rainfall over East Asia. Scientific Reports, 11(1), 13665.

37) Tochimoto, E., & Hirockawa, Y. (2024). Environmental characteristics of an extreme rainfall event in Yamagata-Niigata prefectures, Japan, on 3-4 August 2022. SOLA, 20A-003.

38) Tsuji, H., Takayabu, Y. N., Shibuya, R., Kamahori, H., & Yokoyama, C. (2021). The role of free-tropospheric moisture convergence for summertime heavy rainfall in western Japan. Geophysical Research Letters, 48(18), e2021GL095030.

39) Tsuguti, H., & Kato, T. (2014). Contributing factors of the heavy rainfall event at Amami-Oshima Island, Japan, on 20 October 2010. Journal of the Meteorological Society of Japan. Ser. II, 92(2), 163-183.

40) Tsuguti, H., Seino, N., Kawase, H., Imada, Y., Nakaegawa, T., & Takayabu, I. (2019). Meteorological overview and mesoscale characteristics of the Heavy Rain Event of July 2018 in Japan. Landslides, 16(2), 363-371.

41) Viale, M., Valenzuela, R., Garreaud, R. D., & Ralph, F. M. (2018). Impacts of atmospheric rivers on precipitation in southern South America. Journal of Hydrometeorology, 19(10), 1671-1687.

42) Waliser, D., & Guan, B. (2017). Extreme winds and precipitation during landfall of atmospheric rivers. Nature Geoscience, 10(3), 179-183.

43) Wang, F., Shao, W., Yu, H., Kan, G., He, X., Zhang, D., ... & Wang, G. (2020). Re-evaluation of the power of the Mann-Kendall test for detecting monotonic trends in hydrometeorological time series. Frontiers in Earth Science, 8, 14.

44) Yan, Y., Zhao, T., Ni, G., & Sun, T. (2017). Atmospheric rivers over the Bay of Bengal lead to northern Indian extreme rainfall. International Journal of Climatology, 38(2), 1010-1021.

https://doi.org/10.5194/egusphere-2026-2597
Preprint. Discussion started: 20 May 2026

45) Yoshida, S., Sakai, T., Nagai, T., Seko, H., Kato, T., Shiraishi, K., & Shimizu, S. (2025). Observation of a slanted moisture structure with weak updraft leading to localized heavy rainfalls. Scientific Reports, 15(1), 22979.

46) Zhang, M., Meng, Z., Huang, Y., & Wang, D. (2019). The mechanism and predictability of an elevated convection initiation event in a weak-lifting environment in central-eastern China. Monthly Weather Review, 147(5), 1823-1841.

47) Zhao, N., Manda, A., Guo, X., & Wang, B. (2022). Impacts of moisture supply from the subtropical western Pacific on the subtropical high and the atmospheric river during the heavy rain of 2020 in Japan. Frontiers in Earth Science, 10, 1043093.